Cross sections for electron trapping by condensed SF_6 and C_6H_6 under the influence of different polarizable environments

F. Weik[a],*, L. Sanche[a]

[a]Groupe CRM en Sciences des Radiations, Faculté de médecine, Université de Sherbrooke, Sherbrooke, QC, Canada J1H 5N4

Abstract

If Benzene molecules adsorbed onto or embedded within rare gas solid films are bombarded with low-energy electrons below 2 eV, charge localization is detected. The maximal cross section for electron trapping by Benzene adsorbed in submonolayers on a Kr film has a value of 8.1×10^{-19} cm^2 in contrast to the isolated molecule where the anion is unstable. On a more polarizable Xe film the cross section maximum is enhanced by a factor of four. Electron attachment to submonolayer SF_6 adsorbed on a Kr film yields a cross section of 2.8×10^{-15} cm^2, which is about one order of magnitude lower than the gas-phase value. On a Xe film this value is enhanced by a factor of 1.6 relative to the Kr substrate. The lower cross SF_6^- yield in the condensed phase is attributed to a lower capture cross section. (Int J Mass Spectrom 205 (2001) 299–307) © 2001 Elsevier Science B.V.

Keywords: C_6H_6; SF_6; Resonance stabilization; Polarization; Condensed films; Charging

Introduction

Electron attachment to isolated molecules is a resonant process, which leads to the formation of a transient negative ion (TNI). The fate of the anion depends strongly on its autodetachment lifetime and thermodynamic properties, (e.g., the adiabatic electron affinity and binding energies of the atoms involved). If its configuration is dissociative in the Franck–Condon region and its autodetachment lifetime sufficiently long, then fragmentation can occur. This process is named as dissociative attachment (DA). When the TNI state is nondissociative, autoionization usually occurs unless the TNI possesses a sufficiently long lifetime (i.e., microseconds) to reach a detector in a mass spectrometric experiment.

If the TNI is generated in a close proximity to other molecules, it polarizes the latter, and the polarization energy usually influences the processes described above. This is the case, when molecules are condensed onto or buried within rare gas solid (RGS) films, which are chemically inert. Depending on the position of the dopant molecule in the RGS film the strength of the polarization energy can be modified.

On a RGS film, below the energy threshold for dipolar dissociation, only stable anionic fragments created via DA can be detected in a mass spectrometric experiment, if they possess sufficient kinetic energy to desorb. This is only possible if the amount of energy released by DA into kinetic energy of the stable anion created after the initial attachment is larger than the polarization energy induced by the

anion in the film. Since values of induced polarization energy are near 1 eV for the anions adsorbed on RGS films, their desorption from such a surface at electron energies below 2 eV is rare. Receding fragment anions created by DA usually do not possess enough kinetic energy to overcome the surface polarization energy. There are only a few desorption processes known, for small molecules containing one or more halogen atoms [1,2], where anion desorption occurs below 2 eV.

Even though an ion created in the low energy range (<2 eV) may not be able to desorb, it may be detected as a charge on a film in or on which it is formed, if its lifetime is very long (i.e., ~1 min) or if it is stable. With the knowledge of gas-phase and/or particular cluster data, film charging can often be attributed to anion creation processes. Furthermore, when anions are localized for the time required for charge measurement (i.e., they do not desorb or migrate) the absolute electron attachment cross section can be obtained.

In this article, we compare absolute cross sections for charge trapping by C_6H_6 and SF_6 condensed at the surface and within RGS films. The idea here is to compare electron trapping by molecules that do not dissociate to any considerable extent via DA below 2 eV, but have different electron attachment properties and very different adiabatic electron affinities (EA) in the gas phase. Since for both molecules DA is not the main charge producing mechanism, we can investigate similarities and differences in the mechanism of charge localization without molecular fragmentation and the response to environments of different polarizabilities. The thermodynamic quantity determining the stability of an anion is the EA, which is very different in both molecules. SF_6 has a positive EA of 1.05 eV [3,4] and forms a stable anion in the gas phase after attachment of electrons with thermal and subthermal energies [5–11]. It exhibits one of the largest cross sections known for electron attachment to isolated molecules. In contrast, C_6H_6 has a negative EA of −1.15 eV [12] and does not form a stable anion in the gas phase. However, from electrochemical experiments, benzene anions are well known to exist

in solutions [13,14] where stabilization is due to the polar nature of the surrounding molecules.

Thus, the two molecules are representative of two different electron capture processes in the gas phase. SF_6^- represents the formation of a long-lived (i.e., microseconds) negative ion with a very large electron attachment cross section sharply peaked at 0 eV leading to a metastable anion [5,6]. On the other hand, $C_6H_6^-$ is typical of a transient molecular anion decaying into a vibrationally excited neutral molecule in the gas phase [12]. However, on the surface and within a RGS film both molecules can stabilize electrons having energies much above thermal. RGS films are thus well suited to study the particular stabilization processes in defined and controllable polarizable environments (i.e., by changing the induced polarization energy by deposition of the molecules on the RGS film surface, into a film, or by changing the RGS).

Experiment

The experimental arrangement and method was first described by Marsolais et al. [15] and later improved by Nagesha et al. [16]. We provide only a brief description in this report. The experiments are carried out in an ion pumped UHV vacuum chamber at a pressure of 5×10^{-11} torr. A 10 to 15 monolayer (ML) Krypton or Xenon film is condensed on a polycrystalline platinum foil held at a temperature of 25K with a closed cycle He refrigerator. A submonolayer of 99.8% SF_6 (Praxair) or 99.9% benzene (Aldrich) is condensed onto the RGS film. In some experiments a "sandwich structure" is formed by condensing additional MLs of rare gas on top of the adsorbed molecule. The liquid benzene is degassed by subsequent freeze–pump–thaw cycles. The RGS films serve as a dielectric spacer to screen mirror charge effects induced by the Pt substrate. The thickness of the RGS film and the submonolayer dose of SF_6 or C_6H_6 are measured by dosing a known amount of the gas from a manifold. The calibration of the amount of gas in the manifold is achieved by thermal desorption spectroscopy. With this method, desorption of multilayers can be discriminated from ML desorption, so

that the amount of gas forming a ML (on the Pt substrate) can be estimated. After the measurements the film is evaporated by electrical heating of the Pt substrate.

The electrons emitted by a tungsten filament are energy selected by a trochoidal electron monochromator (TEM) of the type first designed by Stamatovic and Schulz [17]. The TEM uses crossed electric and magnetic fields to disperse electrons with respect to their energies. The magnetic field is orientated in the direction of the electron beam; the latter impinges on the surface at normal incidence. The magnetic field collimates the electron beam and keeps its dimension fairly constant within the low-energy range. Especially near 0 eV, stray electric and magnetic fields influence the electron trajectory. With both energy selection and magnetic collimation, their effect is negligible, the electron beam is stable and very low energies can be reached with energy resolutions below 100 meV. Such conditions are a prerequisite for the measurement of electron trapping cross sections in the condensed phase, which, near 0 eV, require measurement of the current onset curve.

The electron current is measured on the Pt substrate with a nanoampere-to-voltage converter. Its output is fed via an analog-to-digital converter into a computer. Electron trapping due to molecules condensed on a RGS film leads to an increase in the work function of the film, which can be detected by comparing the transmitted current onset of the charged film with that of the uncharged film. With accumulated charge on the film surface or within the film the impinging electrons need a higher energy to transmit to the metal substrate. Thus on a charged film the electron onset shifts to a larger potential difference between the substrate and the monochromator. From this shift ΔV, an electron trapping coefficient A_s is calculated by the formula [15,16]:

$$A_s(E) = \frac{d}{dt} \Delta V(t)\big|_{t=0} = \frac{\rho_0 J_0 L_1 \sigma(E)}{\kappa \varepsilon_0} \times \beta(L_1, L_2, \kappa) \tag{1}$$

where ρ_0 is the initial density of electron trapping molecules on the surface of the RGS film, J_0 is the incident current density, L_1 is the thickness of the

RGS film and κ is the dielectric constant. The latter has a value of 1.91 for the Krypton film and 2.27 for the Xenon film [18]. ϵ_o is the permittivity of free space. In the case of benzene, ρ_0 is taken from a LEED study [19] as 1.9×10^{14} molecules/cm^2 and in the case of SF$_6$ from bulk data [20] as 4.6×10^{14} molecules/cm^2. The function β depends on κ, the thickness L_1 of the RGS layer between the molecule and the metal and the overlayer thickness L_2. In the present experiment for $L_2 > 6$ ML, β converges to the reciprocal of the RGS bulk dielectric constant, that is, 1.91^{-1} for Kr and 2.27^{-1} for Xe and it is equal to unity for $L_2 = 0$ [21].

The experiment is performed by first sweeping the monochromator potential over the current onset of the uncharged film. After the film is exposed to electron irradiation at a fixed electron energy for sufficient time to charge the film at an easily recordable potential. A subsequent measurement of the current onset determines the shift ΔV in Eq. (1) from which the cross section is calculated. The charging time, energy onset measurement and calculation of the trapping cross section are managed by a computer. The absolute uncertainty of the cross sections was estimated to be 50% [16]. The main contribution to the error is from the dosing procedure of the RGS film and the molecules adsorbed on the surface or embedded in the film. An estimated error of 20% applies in each case. The maximal time necessary for one measurement at a given energy is ~approximately 1 min. This means that the trapped charge must be stable on this timescale. No change in the numbers of charges was observed during the time of the measurements.

Results and discussion

Benzene

The cross section for electron trapping due to the presence of 0.1-ML benzene condensed on the surface of an 11-ML-thick Kr layer is shown in Fig. 1a. The cross section for 0.1-ML benzene isolated within a Kr film is displayed in Fig. 1b. The benzene dosage and L_1 are kept constant in both measurements. The data
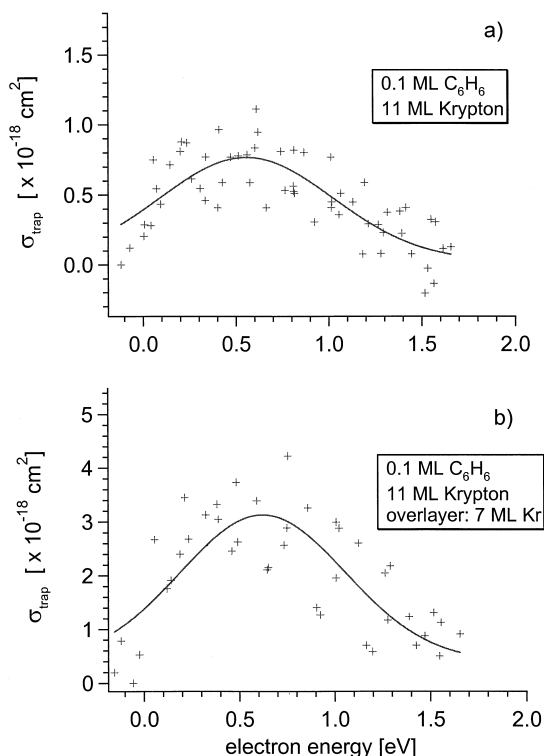
FIG. 1.(a) Electron trapping cross section for 0.1-ML benzene adsorbed on a 11-ML Kr film. (b) Electron trapping cross section for 0.1-ML benzene adsorbed on a 11-ML Kr film and a similar film covered with an overlayer of 7-ML Kr.

in Fig. 1b is obtained by dosing 7 ML of Kr on top of the benzene submonolayer. Both graphs contain gaussian fits to the data points to show the resonance profile.

In the case of a submonolayer dose of benzene on the Kr film, a cross section maximum of 8.1×10^{-19} cm^2 at the energy of 0.6 eV is derived from the maximum of the gaussian fit to the data points. This value is four times smaller than the cross section maximum of 3.2×10^{-18} cm^2 obtained from the sandwich structure (Fig. 1b). The electron-trapping cross section for 0.1 ML of benzene condensed onto 10 ML of Xenon is shown in Fig. 2. The maximum of the gaussian fit is located around 0.7 eV. The cross section value of 3.2×10^{-18} cm^2 is four times larger than the data from the Kr film surface and equals the value from the Kr sandwich structure.

Electron attachment to isolated Benzene molecules produces an anionic resonance with a vibrational progression detected by electron transmission spectroscopy between 1.1 eV and 1.8 eV [12,14,22]. The transient anion, with $^2E_{2u}$ symmetry is attributed to electron attachment to the π^* virtual molecular orbital. This symmetry is connected to the totally symmetric "ring-breathing" vibration mode. The negative value of (-1.15 ± 0.05) eV [12] of the EA indicates that the isolated anion is unstable to autodetachment.

The resonance profiles in the data sets of Figs. 1 and 2 are showing maxima around 0.6 eV, which are 0.55 eV lower than the strongest resonant feature of the vibrational progression in the gas phase, lying at a vertical attachment energy of 1.15 eV [12]. A polarization energy of 0.72 eV found by Michaud and Sanche [18] for the lowest N_2^- resonance on a Kr film fits fairly well with a shift of the gas phase ^2E_u anion state to lower energy by induced polarization. However, a further shift, as expected from the larger bulk polarization in the sandwich structure (i. e., 1.15 eV [18]) is not observed. This may be due to the fairly high scattering of the data, which makes the detection of a possible shift of the maximum difficult on a scale of a few 100 meV. Thus we interpret the maxima in Figs. 1 and 2 as due to the ^2E_u state of the benzene anion. Electrons incident on the Kr or Xe surface are

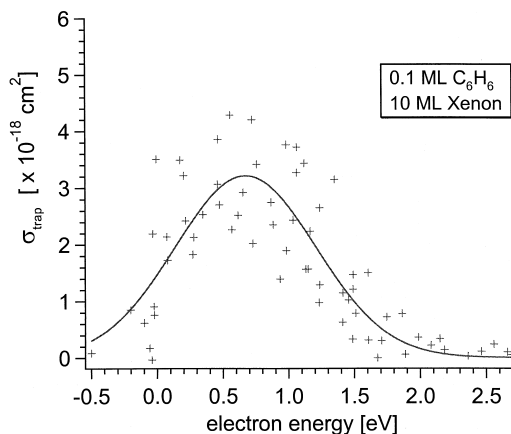FIG. 2. Electron trapping cross section for 0.1-ML benzene adsorbed on a 11-ML Xe film.

captured by C_6H_6 to form the ^2E_u anion configuration, which means at the surface and within the bulk C_6H_6 has a negative electron affinity of about -0.5 to -0.6 eV. This makes the stabilization of a negative charge on and within the RGS film surprising, since to produce a measurable charge the anion must be present on or within the film for times required for the measurements (i.e., minutes).

In solutions, the benzene anion is well known to exist [13,14], but only in polar solvents, which yield total polarization energies of usually several electron volts are necessary to stabilize the lowest ^2E_u anion state of C_6H_6. However, in RGS films with only electronic polarization reorganization of dipoles is not present to stabilize the ^2E_u state. But even without the presence of polar solvents one could envisage reorganization of the initial ^2E_u benzene anion configuration to a configuration with a parent neutral state of positive EA. This requires that the lifetime of the initial ^2E_u state has to increase sufficiently in the condensed phase, to allow for a change of the anion geometry, most probably of the carbon ring. Such a stabilization mechanism was found in CO_2, which form stable CO_2^- after electron attachment around 4 eV in clusters, but not in the isolated molecule [23,24]. Similarly, in surface electron trapping experiments performed with the apparatus used in this study, it was found that the gas phase 4 eV CO_2^- ($^2\Pi_u$) could be stabilized around 3 eV on a Kr film [25]. The CO_2^- yield was attributed to the formation of a bent CO_2 configuration [25].

On the other hand, among benzene–water clusters, the benzene–water–hexamer was observed as the dominant contribution in the cluster signal [26]. A comparison of the photoelectron spectrum of this anionic cluster with the pure anionic water–hexamer revealed a much higher binding energy of the excess electron for the benzene–water–hexamer. This led to the conclusion that a cluster trapping mechanism could cause electron scavenging even if the impurity molecule has a negative electron affinity. Similarly, in the present case, electron stabilization can also be considered by taking into account the characteristics of the RGS film. The incoming electron can first be trapped in the π^* virtual molecular orbital of the

benzene molecule as in the gas phase, and this state can act as a precursor to another subsequently formed final state trapping the electron permanently or retaining it for minutes. The final state may be connected to dislocations or impurities in the RGS film itself, which are not accessible when C_6H_6 is not present. Both produce distortions in the periodic potential of the RGS lattice, in which localized states could exist below the minimum of the conduction band V_0 of the RGS film (i.e., below the V_0 of Kr and Xe films located at -0.25 eV and -0.45 eV [27], respectively, relative to the vacuum level). Such states are therefore not accessible for electrons incoming in the pure RGS thin films in which energy losses to phonons are minimal. Thus, no electron trapping is observed in pure RGS films with thicknesses around 10 ML. With benzene on the film surface or in the bulk, the incoming electron could loose energy more efficiently via vibrational excitation and fall into trapping sites below the vacuum level; particularly, by decay of the ^2E_u resonance directly into the gap state. In this case, the electron would be trapped into dislocation or impurity states, thus leading to the observed charging profile. The higher cross section of the sandwich structure could be explained by the lower probability of back-scattered electrons escaping into the vacuum because the scattering event occurs within the film. On xenon films the number of dislocations should be higher because the dosing temperature is further away from the melting point than for Kr films. Therefore the density of trapping states should be higher in the more disordered solid (i.e., Xe), leading to a higher cross section for the electron localization.

Finally, one could remark that the cluster and surface mechanisms may be similar. In clusters the benzene molecule creates a new state for electron trapping in the cluster, whereas in the film the trapping state can possibly be created by an impurity state, caused by the presence of the benzene molecule within the band structure of the rare gas film.

Sulphurhexafluoride

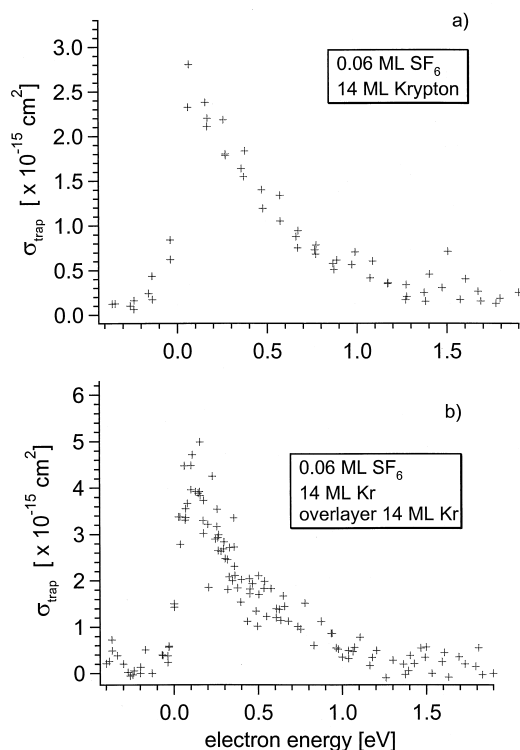The electron trapping cross section for 0.06 ML SF_6 on a 14-ML Kr film is displayed in Fig. 3a. A

FIG. 3.(a) Electron trapping cross section for 0.06-ML SF$_6$ adsorbed on a 14-ML Kr film. (b) Electron trapping cross section for 0.06-ML SF$_6$ condensed between two Kr layers of 14-ML thickness.

maximal value of 2.8×10^{-15} cm^2 for the cross section is found at an electron energy of 65 meV, but a high energy tail extends up to 1 eV. These results are similar to those of a recent study on electron attachment to molecules in Ar clusters and adsorbed on RGS films [28]. The charge localization is due to electron attachment to SF$_6$ at near 0 eV energy leading to stable and long-lived SF$_6^-$. This process is well known from gas phase studies [5,6]. Cross sections from 1.0×10^{-14} cm^2 [8] to 3.6×10^{-14} cm^2 [9] are found in high-pressure swarm experiments at thermal electron energies (i.e., 27 meV). These values are about one order of magnitude larger than the condensed phase cross section reported in Fig. 3a. Even higher cross sections with values up to 10^{-13} cm^2 are found in the gas phase with electron resolutions near 5 meV [11].

The accepted value for the electron affinity of SF$_6$

is (1.15 ± 0.15) eV [29]. It indicates that stable SF$_6^-$ can be formed in the gas by multiple-body collisions. The relatively large vertical detachment energy (VDE) of 3.16 eV, measured in a photodetachment experiment [30], suggests that a fairly large change in molecular dimensions takes place between the neutral molecule geometry and the negative ion in its relaxed geometry. Theoretical calculations predict the relaxed anionic geometry to be the same as the O_h symmetry of the neutral with an enlargement of all S—F bonds by 9% with respect to the internuclear distance of the neutral [31]. Such a large change in bond length must lead to a highly vibrationally excited anion upon electron attachment.

The anion signal measured in the gaseous electron beam experiments is confined to values near 0 eV. The signal width is limited by the resolution of the electron monochromator [7]. In fact, an application of the sharp SF$_6^-$ signal near 0 eV is to be found in the first measurements of the energy resolution of the TEM by its inventors Stamatovic and Schulz [17].

As seen in Fig. 3a, under the influence of a polarizable environment the SF$_6^-$ signal shows the previously mentioned extension to higher electron energies also seen in clusters [28]. In the latter case, the signal extension can be explained by a stabilization of the anion due to evaporation of the cluster. Such a mechanism is efficient to dissipate excess energy brought into a cluster [32]; that is, vibrationally hot SF$_6$ anions are cooled to lower vibrational states by coupling to phonon modes of the cluster. Energies up to ~1 eV can be dissipated by cluster evaporation.

With thin films, such a mechanism is also possible. Because of the symmetry of the SF$_6$ molecule, any distortion of the geometry due to electron attachment produces a vibrational mode having a component normal to the RGS surface which can couple well to the phonon bath of the RGS film [28]. Thus an effective and rapid dissipation of SF$_6^-$ vibrational energy is operative for the molecules on the Kr surface [28] leading to SF$_6^-$ stabilization up to energies of ~1 eV.

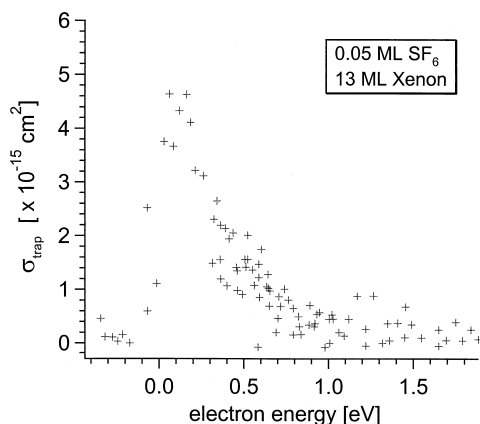These arguments should be even more valid when the SF$_6$ molecule is confined within a RGS film. The

FIG. 4. Electron trapping cross section for 0.05-ML SF_6 adsorbed on a 13-ML Xe film.

attachment coefficients measured from 0.06 ML of SF_6 embedded between two Kr layers of 14 ML thickness (i.e., the sandwich structure) is displayed in Fig. 3b. It shows the same shape as in Fig. 3a; that is, a curve of the attachment cross section with the high-energy tail extending up to 1 eV. The maximum of the cross section is 5.0×10^{-15} cm^2, nearly twice that of 2.8×10^{-15} cm^2 found on the Kr surface.

In order to investigate the effect of polarization, we changed the RGS from krypton to xenon. In Fig. 4 the cross section for 0.05-ML SF_6 condensed on 13-ML Xe is displayed. Its maximum value is 4.6×10^{-15} cm^2; it is by a factor of 1.6 larger than the value of the maximum measured on the Kr film. Thus, a change in polarization energy when going from the Kr to the Xe film (i.e., from 0.72 eV to 0.89 eV, respectively) obviously does not alter the cross section significantly. This behavior is in contrast to earlier studies on CF_3Cl [33] and CH_3Cl [34] condensed on and within Kr films. In these cases, the change in polarization energy has a large effect on the stable anion formation cross section. It was enlarged by one order of magnitude for CF_3Cl and by five to six orders of magnitude in the case of CH_3Cl compared to the isolated molecule. However with these molecules the charging process was due to DA. In this case, the huge enhancement in the cross section for stable anion formation could be explained by considering that the DA cross section σ_{DA} can be expressed as the product

of the survival probability P and the electron capture cross section σ_c [35]; namely,

$$\sigma_{DA} = \sigma_c \times P. \tag{2}$$

As described previously [33,36,37], P can increase considerably when the induced polarization energy reduces the energy of the anion state. This is the case for CF_3Cl and CH_3Cl, which causes a corresponding increase in the DA cross section σ_{DA}. However, for electron stabilization on the parent molecule, P is not in consideration and near 0 eV σ_c becomes the controlling factor. Thus, as seen here for SF_6, increasing the polarization induced at the surface has little effect on σ_{DA}. However, σ_c contains a term directly proportional to the square of the electron wavelength [35]. The latter is huge at 0 eV in the gas phase, whereas for an electron impinging on a surface it is necessarily much smaller since polarization increases momentum close to the surface. Thus, we expect a larger attachment cross section to gaseous SF_6 than to adsorbed SF_6. This is also reflected in the E^{-1} behavior of DA cross section for energies E around 100 meV for gaseous CCl_4 [38]. Since in this case $P \cong 1$ in Eq. (2), the condensed phase cross section for DA to CCl_4 near 0 eV is, as in the present case of SF_6, found to be smaller, that is, about a third of the gas phase value [39]. Thus, it appears that for both DA and resonance stabilization on the parent molecule, acceleration of the electron near the film surface increases its momentum, and therefore the very low energy attachment processes present in the gas phase may not be reached, even if they are accessible within the resolution of the experiment (<100 meV). This explains the smaller maximum value of the SF_6^- cross section compared to the gas phase values, but our qualitative arguments are not sufficiently accurate to explain small differences in cross sections in the different condensed environments (i.e., Kr surface, Kr sandwich, and Xe surface).

Finally, we note that the SF_6 anion, with its already positive EA in gas phase, only needs an effective way of decreasing its vibrational excess energy, to stabilize in the condensed phase. Although this is possible on or within both RGS films, the decrease of the cross

section with increasing electron energy is faster on the Xe surface. This behavior means that the vibrational energy transfer to phonons, needed to stabilize the anion, is less efficient on the Xe film so that beyond ~0.8 eV autoionization occurs predominantly. For a highly excited anion this transfer must contain several vibrational quanta, each of which needs to be transferred via multiphonon processes. The RGS films are dosed at the same temperature of 25K. For Xe this growth temperature is much lower than the melting point, leading to a higher amount of faults and dislocations in the crystal than for Kr. These defects lead to a modification and possibly a decrease of the phonon density of states of the Xe lattice. The smaller phonon density of states could diminish energy transfer from anions to the extent that autodetachment, as a decay channel of the resonance, takes over stabilization at the higher energies.

Conclusion

The ground state C_6H_6 ^2E_u anion, with a negative electron affinity, is thermodynamically not stable in the gas phase. When formed on Kr and Xe RGS films, however, it produces a profile in the charging coefficient that exhibits a shape typical of an anionic resonance. It's maximum is lowered by an amount of energy that is very close to the polarization energy of the Kr RGS film. From the charging data, a maximal cross section of 8.1×10^{-19} cm^2 is found for electron trapping via C_6H_6 adsorbed on a Kr film. This value is enhanced by a factor of four when the benzene molecule is adsorbed on a Xe layer instead of Kr. We explain this enhancement mainly by an increase of the density of trapping states due to a greater disorder of the Xe film compared with the Kr film.

The SF_6 anion, with a positive EA, is stabilized up to energies of ~1 eV, in contrast with the gas phase where the SF_6^- peak is confined around 0 eV. A maximum electron attachment cross section of 2.8×10^{-15} cm^2 is measured with submonolayers of SF_6 adsorbed onto a Kr surface. This value is about one order of magnitude smaller than the gas-phase value. The maximum of the cross section is enhanced

by a factor of 1.6 on a Xe surface. This shows that the stronger polarization interaction of the Xe film compared to the Kr film does not effect the cross section values significantly. Stabilization takes place from 0–1 eV due to rapid dissipation of vibrational energy to the RGS film.

This article, along with others [40], illustrates an application of the trochoidal monochromator devised by Stamatovic and Schulz [17], in the field of surface science—namely, the use of low energy electron transmission spectroscopy (LEET) in condensed film to measure absolute trapping cross sections at surfaces and within solids. It may be interesting to note that the first widespread application of the TEM was the development of electron transmission spectroscopy in the gas phase [12,14,41].

Acknowledgement

References

[1] P. Tegeder, E. Illenberger, Phys. Chem. Chem. Phys. 1 (1999) 5197.
[2] P. Rowntree, L. Sanche, L. Parenteau, M. Meinke, F. Weik, E. Illenberger, J. Chem. Phys. 101 (1994) 4248.
[3] E.P. Grimsrud, S. Chowdhury, P. Kebarle, J.Chem.Phys. 83 (1985) 1059.
[4] E.C.M. Chen, J.R. Wiley, C.F. Batten, W.E. Wentworth, J. Phys. Chem. 98 (1994) 88.
[5] W.M. Hickam, R.E. Fox, J. Chem. Phys. 25 (1956) 642.
[6] M. Fenzlaff, E. Illenberger, Chem. Phys. 136 (1989) 443.
[7] S. Matejcik, P. Eichberger, B. Plunger, A. Kiendler, A. Stamatovic, T.D. Maerk, Int. J. Mass Spec. Ion Proc. 144 (1995) L 13–L 17.
[8] D.L. McCorkle, A.A. Christodoulides, L.G. Christophorou, I. Szamrej, J. Chem. Phys. 72 (1980) 4049.
[9] F.J. Davis, R.N. Compton, D.R. Nelson, J. Chem. Phys. 59 (1973) 2324.
[10] D. Smith, N.G. Adams, E. Alge, J. Phys. B 17 (1984) 461.
[11] D. Klar, M.-W. Ruf, H. Hotop, Chem. Phys. Lett. 189 (1992) 448.
[12] P.D. Burrow, J.A. Michejda, K.D. Jordan, J. Chem. Phys. 86 (1987) 9.

[13] J. Mortensen, J. Heinze, Angew. Chem. Int. Ed. Engl. 23 (1984) 84.

[14] I. Nenner, G.J. Schulz, J. Chem. Phys. 62 (1975) 1747.

[15] R.M. Marsolais, M. Deschênes, L. Sanche, Rev. Sci. Instr. 60 (1989) 2724.

[16] K. Nagesha, J. Gamache, A.D. Bass, L. Sanche, Rev. Sci. Instr. 68 (1997) 3883.

[17] A. Stamatovic, G.J. Schulz, Rev. Sci. Instr. 41 (1970) 423.

[18] M. Michaud, L. Sanche, J. Elec. Spec. Rel. Phen. 51 (1990) 237.

[19] P.C. Stair, G.A. Somorjai, J. Chem. Phys. 67 (1977) 4361.

[20] A.P. Isakina, A. I. Prokhvatilov, Low. Temp. Phys. 19 (1993) 142.

[21] K. Nagesha, L. Sanche, unpublished.

[22] L. Sanche, G.J. Schulz, J. Chem. Phys. 58 (1973) 479.

[23] C.E. Klots, R.N. Compton, J. Chem. Phys. 69 (1978) 1636.

[24] A. Stamatovic, K. Leiter, W. Ritter, K. Stepan, T. D. Märk, J. Chem. Phys. 83 (1985) 2942.

[25] M.A. Huels, A.D. Bass, P. Ayotte, L. Sanche, Chem. Phys. Lett. 245 (1995) 387.

[26] T. Maeyama, T. Oikawa, K. Seguchi, N. Mikami, J. Phys. Chem. A 101 (1997) 8371.

[27] L.G. Caron, G. Perluzzo, G. Bader, L. Sanche, Phys. Rev. B 33 (1986) 3027.

[28] F. Weik, O. Ingólfsson, L. Sanche, E. Illenberger, J. Chem. Phys., 112 (2000) 9046.

[29] E.C.M. Chen, L.-R. Shuie, E.D. D'sa, C.F. Batten, W.E. Wentworth, J. Chem. Phys. 88 (1988) 4711.

[30] P.G. Datskos, J.G. Carter, L.G. Christophorou, Chem. Phys. Lett. 239 (1995) 38.

[31] R.A. King, J.M. Galbraith, H.F. Schaefer III, J. Phys. Chem. 100 (1996) 6061.

[32] C.E. Klots, Radiat. Phys. Chem. 20 (1982) 51.

[33] K. Nagesha, L. Sanche, Phys. Rev. Lett 78 (1997) 4725.

[34] L. Sanche, A.D. Bass, P. Ayotte, I.I. Fabrikant, Phys. Rev. Lett 78 (1997) 4725.

[35] T. F. O'Malley, Phys. Rev. 150 (1966) 14.

[36] H. Sambe, D.E. Ramaker, M. Deschênes, A.D. Bass, L. Sanche, Phys. Rev. Lett. 64 (1990) 523.

[37] A.D. Bass, J. Gamache, L. Parenteau, L. Sanche, J. Phys. Chem. 99 (1995) 6123.

[38] S. Matejcik, A. Kiendler, A. Stamatovic, T.D. Märk, Int. J. Mass Spectrom. Ion Proc. 149/150 (1995) 311.

[39] A.D. Bass, J. Gamache, P. Ayotte, L. Sanche, J. Chem. Phys. 104 (1996) 4258.

[40] A.D. Bass, L. Sanche, Radiat. Environ. Biophys. 37 (1995) 243, review article.

[41] L. Sanche, G.J. Schulz, Phys. Rev. Lett. 26 (1971) 943.